AIMS Mathematics, 10(11): 28059–28076.
DOI: 10.3934/math.20251233
Received: 07 August 2025
Revised: 29 October 2025
Accepted: 12 November 2025
Published: 28 November 2025

https://www.aimspress.com/journal/Math

Research article

Feedback-driven strategies for controlling infectious outbreaks

Mohammed Azoua[1], Marouane Karim[2], Amine Rachih[3], Mostafa Rachik[2], and Mahmoud A. Zaky[4,*]

[1] Laboratory of Process Engineering Computer Science and Mathematics, University Sultan Moulay Slimane, BeniMellal, Morocco

[2] Multidisciplinary Research and Innovation Laboratory (LPRI), Moroccan School of Engineering Sciences (EMSI), Casablanca 20250, Morocco

[3] Laboratory of Analysis Modelling and Simulation, Department of Mathematics and Computer Science, University Hassan II , Casablanca, Morocco

[4] Department of Mathematics and Statistics, College of Science, Imam Mohammad Ibn Saud Islamic University (IMSIU), Riyadh 11566, Saudi Arabia

* **Correspondence:** Email: ma.zaky@yahoo.com, mibrahimm@imamu.edu.sa.

Abstract: In response to the global health crises posed by infectious diseases like COVID-19, this study presents an enhanced SEIR model by introducing a novel feedback control mechanism. This mechanism dynamically adapts not only to the current state of the infected population but also to its rate of change, offering a dual-dependence control strategy. Such an approach significantly enhances the responsiveness and precision of epidemic management interventions, leading to a substantial reduction in peak infection rates and overall disease burden. To achieve optimal control, we employed the gradient descent method for mathematical analysis, ensuring both theoretical robustness and computational efficiency. Theoretical results were validated through comprehensive numerical simulations, demonstrating the efficacy of our control strategy across various epidemic scenarios. Furthermore, a comparative analysis with Pontryagin's maximum principle highlights the superior performance of our model, underscoring the critical role of incorporating both state and rate of change information in designing effective public health interventions. These findings reveal new possibilities for improving epidemic containment strategies, offering valuable insights for real-world disease management.

Keywords: epidemiological model; feedback control; adjoint sensitivity method; optimal control
Mathematics Subject Classification: 49Jxx, 49Kxx, 93Axx, 93Cxx

1. Introduction

Infectious diseases remain a persistent threat to global public health, as dramatically illustrated by recent outbreaks, including the COVID-19 pandemic. Such events have underscored the crucial need for effective tools to analyze and mitigate the spread of contagious pathogens. Among these tools, mathematical models have proven to be indispensable in understanding disease transmission dynamics and in guiding policy decisions. In particular, compartmental models, such as the classical susceptible–infectious–recovered (SIR) model introduced by Kermack and McKendrick in 1927 [2], have laid the foundation for the development of more elaborate frameworks. One such refinement is the susceptible–exposed–infectious–recovered (SEIR) model, which incorporates a latent phase to account for the incubation period characteristic of many infectious diseases [6–8].

Despite the wide adoption of these models, a major limitation persists: The inability to dynamically adjust intervention strategies in response to the evolving state of an epidemic. Traditional approaches typically rely on static or pre-planned controls, which can be insufficient in rapidly changing contexts. This challenge has prompted a growing interest in the integration of feedback mechanisms within epidemic models, allowing control measures to adapt in real time based on the system's behavior [9–12]. Feedback control offers a pathway toward more resilient and efficient public health responses by continuously tuning interventions to match the epidemic's progression.

Various feedback strategies have been explored in the literature, including vaccination, treatment policies, and non-pharmaceutical interventions. However, many existing models employ simplistic feedback schemes that react solely to the current level of infection without considering the temporal trends or rate of change in disease prevalence [13, 14, 21]. Such approaches may fail to capture the urgency required in the face of rapidly escalating outbreaks. Furthermore, it has also been shown that behavioral and information-related effects, such as the influence of messages disseminated on social media on the spread of the epidemic, have a significant impact on transmission dynamics [22].

In this work, we propose an enhanced $SEIR$-type model that introduces a novel feedback control mechanism. Unlike conventional methods that rely only on the instantaneous number of infected individuals, our approach simultaneously incorporates the rate of change of infections. This dual-dependence control strategy, based on both the infection level $I(t)$ and its time derivative $I'(t)$, enables a more agile and anticipatory response to shifts in epidemic trends. The resulting control scheme is thus better equipped to mitigate sudden surges in infections and to stabilize disease dynamics more effectively.

The motivation for this study lies in the observed shortcomings of traditional control frameworks, particularly their inability to respond proactively to changing epidemiological conditions. By leveraging real-time information about the growth rate of infections, the proposed feedback law provides a significant advantage in responsiveness and control precision. This has practical implications for the timely implementation of containment strategies, especially during early outbreak phases or in the presence of new variants.

To assess the effectiveness of our methodology, we perform a comparative analysis with the classical optimal control approach rooted in Pontryagin's maximum principle [15–17]. Many studies also extend these methods to more general frameworks, notably fractional optimal control approaches [5]. This principle has long been a standard in determining time-dependent intervention strategies in epidemiology. Our findings reveal that the feedback-based approach offers tangible benefits in terms

of adaptivity, robustness, and computational efficiency.

In summary, this paper contributes to the advancement of epidemic modeling by introducing a feedback control strategy that adapts to both the state and the dynamics of infection spread. The proposed model not only extends the theoretical understanding of control in compartmental systems, but also provides practical tools for decision-makers facing the challenges of epidemic containment.

The remainder of this paper is structured as follows. In Section 2, we introduce the mathematical formulation of the SEIRS model and provide the foundational analysis. Section 3 presents the controlled version of the model and details the design of the feedback mechanism. Section 4 is devoted to the training via adjoint sensitivity analysis. In Section 5, we formulate and solve the optimal control problem using Pontryagin's framework. Section 6 offers a comparative study between the proposed feedback method and classical optimal control strategies. Finally, we summarize the key insights and discuss potential extensions in Section 7.

2. Problem statement

In order to understand the mechanisms behind the spread of infectious diseases and to create successful intervention methods, mathematical modeling is essential [18, 19]. The SEIRS framework is unique among the other compartmental models used in epidemiology since it introduces an exposed class to capture the incubation time. In order to appropriately represent diseases where recovered patients may re-infected, we propose an enhanced SEIRS model in this study that takes waning immunity into account.

The complex interactions between the population compartments are reflected in our model, which is built under biologically plausible assumptions. In particular, we establish four groups from the entire population $N(t)$ at time t: susceptible people $S(t)$, exposed individuals $E(t)$, infectious individuals $I(t)$, and recovered individuals $R(t)$. The behavior of the system is described by the following set of nonlinear ordinary differential equations:

$$\begin{cases} S'(t) = \Lambda - \alpha S(t)\dfrac{I(t)}{N(t)} + \theta R(t) - dS(t), \\ E'(t) = \alpha S(t)\dfrac{I(t)}{N(t)} - aE(t) - dE(t), \\ I'(t) = aE(t) - (g + r + d)I(t), \\ R'(t) = gI(t) - \theta R(t) - dR(t), \end{cases} \tag{2.1}$$

with nonnegative initial conditions $S(0), E(0), I(0), and\ \ R(0) \geq 0$. According to Table 1, every system parameter records a significant biological or epidemiological process.

Table 1. Descriptions of the parameters used in the model.

Parameters	Descriptions
Λ	Coefficient of the recruitment rate
α	Infection rate coefficient
d	Coefficient of the natural mortality rate
r	Coefficient of the mortality due to the virus
a	Inverse of the average incubation period of the disease
g	Coefficient of the recovery intensity of infected individuals
θ	Loss rate of immunity

The entire population is described by $N(t) = S(t) + E(t) + I(t) + R(t)$. The phase space of permissible state variables is introduced to make the analysis easier:

$$\mathcal{X} := \left\{x = (S, E, I, R) \in \mathbb{R}^4_+ : S(t) + E(t) + I(t) + R(t) = N(t), \forall t \geq 0\right\}.$$

The nonnegativity of the model solutions is an important first finding that guarantees the model's epidemiological relevance.

Theorem 2.1. *(Positivity of Solutions) Let $(S(t), E(t), I(t), R(t))$ be a solution to system (2.1) with nonnegative initial conditions. Then, for all $t \geq 0$, the components $S(t), E(t), I(t), R(t)$ remain nonnegative.*

Proof. See [15] for a detailed proof. □

Furthermore, by adding the equations in (2.1), we obtain the population dynamics:

$$N'(t) = \Lambda - dN(t) - rI(t).$$

This implies that the population as a whole is eventually bounded. In other words, if $N_0 = N(0)$, then:

$$N(t) \leq N_0 e^{-dt} + \frac{\Lambda}{d} \leq K,$$

where $K = N_0 + \Lambda/d$, and hence:

$$S(t), E(t), I(t), R(t) \leq K, \quad \forall t \geq 0.$$

Remark 2.2. The boundedness of $N(t)$ implies that all compartments in the system are uniformly bounded by the constant K.

We normalize the system by dividing each compartment by $N(t)$ in order to simplify the mathematical analysis. We determine the system's normalized form assuming a constant population size:

$$\begin{cases} S'(t) = \Lambda - \alpha S(t)I(t) + \theta R(t) - dS(t), \\ E'(t) = \alpha S(t)I(t) - aE(t) - dE(t), \\ I'(t) = aE(t) - (g + r + d)I(t), \\ R'(t) = gI(t) - \theta R(t) - dR(t). \end{cases} \tag{2.2}$$

Letting $S(t) + E(t) + I(t) + R(t) = 1$, the normalized state space becomes:

$$\mathcal{X} := \left\{ x = (S, E, I, R) \in \mathbb{R}^4_+ : S(t) + E(t) + I(t) + R(t) = 1, \forall t \geq 0 \right\}.$$

The existence of solutions for system (2.2) is the next topic we discuss. Rewriting it in the conventional Cauchy form:

$$\begin{cases} x'(t) = f(t, x), \\ x(0) = x_0. \end{cases}$$

The vector field f can be divided into two parts: A linear and a nonlinear component as follows:

$$f(t, x) = \mathcal{M}x + \mathcal{H}(x),$$

where

$$\mathcal{M} = \begin{pmatrix} -d & 0 & 0 & \theta \\ 0 & -(a+d) & 0 & 0 \\ 0 & a & -(g+r+d) & 0 \\ 0 & 0 & g & -(d+\theta) \end{pmatrix}, \quad \mathcal{H}(x) = \begin{pmatrix} \Lambda - \alpha S I \\ \alpha S I \\ 0 \\ 0 \end{pmatrix}.$$

The existence and uniqueness of solutions are ensured by the standard Cauchy–Lipschitz theorem, which makes it simple to confirm that f is locally Lipschitz continuous.

3. Control design and optimization framework

We provide a feedback control mechanism that is directly included into the SEIRS model's structure to improve the responsiveness of intervention tactics against epidemic outbreaks. By using real-time data regarding the infection dynamics, particularly the state variable $I(t)$ and its rate of change $I'(t)$, this method goes beyond conventional time-dependent or state-only control approaches. This decision was made in order to produce a control legislation that is sensitive to sudden changes in the spread of illness and adaptable.

3.1. Feedback-driven controlled model

The design of a feedback-based control mechanism incorporated into the SEIRS framework is a significant innovation of this study. The suggested approach presents a dynamic control rule that adjusts in real time to the current infection condition and its progression, in contrast to traditional control techniques that recommend fixed actions or optimize predetermined control functions offline. In particular, the model is expanded by adding a control input $u(t)$ that adjusts the rate at which infected people are removed, signifying the severity of interventions like treatment, isolation, or other health regulations. This is how the controlled SEIRS system is constructed:

$$\begin{cases} S'(t) = \Lambda - \alpha S(t)I(t) - dS(t) + \theta R(t), \\ E'(t) = \alpha S(t)I(t) - (a+d)E(t), \\ I'(t) = aE(t) - (g+r+d+u(t))I(t), \\ R'(t) = (g+u(t))I(t) - (\theta+d)R(t). \end{cases} \tag{3.1}$$

The control $u(t)$ is expressed as a feedback function of the number of people infected at a given moment and the rate at which this number changes:

$$u(t) = k_1(t)I'(t) + k_2(t)I(t), \tag{3.2}$$

where the time-dependent gain functions $k_1(t)$ and $k_2(t)$ establish how sensitive the control is to infection dynamics. This formulation incorporates important epidemiological data and offers a number of benefits:

- **Responsiveness to acceleration:** The trend in infection rates is captured by the derivative term $I'(t)$. The control automatically increases when infections are increasing quickly (i.e., $I'(t) \gg 0$), allowing for the prompt scaling up of interventions like mass testing, more stringent isolation, or emergency treatment mobilization.
- **Proactive control:** By identifying early indicators of acceleration, this control predicts future load, in contrast to reactive techniques that simply react to current levels $I(t)$. Avoiding system delays is essential, since previous pandemics like COVID-19 have shown that even a few-day delay in intervention can have disastrous results.
- **Stabilization in post-peak phases:** The control automatically decreases when the epidemic slows (i.e., $I'(t) < 0$), preventing needless or excessive restrictions. This permits the reallocation of resources or the relaxation of public measures without sacrificing safety.

This control structure can be viewed as a **generalization of proportional-derivative (PD) controllers** used in engineering systems, where $I(t)$ acts as the proportional component and $I'(t)$ as the derivative. Its application in epidemic control offers a powerful and interpretable tool: When the epidemic is stable ($I'(t) \approx 0$), the intervention intensity depends mostly on the current prevalence. When the epidemic begins to surge, the derivative term triggers a rapid increase in control pressure, effectively **buying time** and **flattening the curve**.

By embedding this control directly into the dynamic system, we establish a framework that is not only mathematically sound, but also grounded in practical realities. This makes the proposed model particularly valuable for **real-time epidemic management**, where quick and data-responsive decisions are essential.

3.2. Objective functional and control constraints

Our goal is to determine the optimal pair of functions $K = (k_1, k_2)$ that minimizes an objective functional reflecting both epidemiological outcomes and control effort. Specifically, we consider:

$$J(x, K) = \int_0^{t_f} \mathcal{G}(x, K)\, dt,$$

where the cost integrand is defined as:

$$\mathcal{G}(x, K) = I(t) - R(t) + \frac{1}{2}c_1 k_1(t)^2 + \frac{1}{2}c_2 k_2(t)^2.$$

The first term penalizes the prevalence of infections while rewarding recoveries, and the last two terms regularize the control effort to avoid extreme interventions. We seek an optimal control $K^* = (k_1^*, k_2^*)$ such that:

$$J(x, K^*) = \min_{K \in \mathcal{K}} J(x, K),$$

where the admissible control set $\mathcal{K}$ is given by:

$$\mathcal{K} := \left\{ (k_1(t), k_2(t)) : 0 \leq u(t) \leq 1, \ \forall t \in [0, t_f] \right\}.$$

3.3. Adjoint-based gradient computation

First, we express the system (3.1) explicitly, as the introduction of the feedback law into the dynamics induces an implicit dependence of $I'(t)$ on the control variables, and consequently on (k_1, k_2), so we define:

$$D(t) := 1 + k_1 I(t), \qquad A(t) := aE(t) - (g + r + d)I(t) - k_2 I(t)^2.$$

The explicit equation for $I'(t)$ is:

$$I'(t) = \frac{A(t)}{D(t)} = \frac{aE - (g + r + d)I - k_2 I^2}{1 + k_1 I},$$

and the explicit control is given by:

$$u(t) = k_1 I'(t) + k_2 I(t) = k_1 \frac{A(t)}{D(t)} + k_2 I(t). \tag{3.3}$$

So, system (3.1) could be rewritten as:

$$\begin{cases} S'(t) = \Lambda - \alpha S I - dS + \theta R, \\ E'(t) = \alpha S I - (a + d)E, \\ I'(t) = \dfrac{aE - (g + r + d)I - k_2 I^2}{1 + k_1 I}, \\ R'(t) = (g + u)I - (\theta + d)R. \end{cases} \tag{3.4}$$

To solve the optimal control problem, we apply a gradient-based optimization strategy. The problem can be rewritten in the standard form:

$$\begin{cases} \min\limits_{K \in \mathcal{K}} \int_0^{t_f} \mathcal{G}(x, K)\, dt, \\ \text{subject to: } x'(t) = f(x, K), \quad x(0) = x_0. \end{cases}$$

We define the Lagrangian functional:

$$\mathcal{L}(x, \lambda, K) = \int_0^{t_f} \left(\mathcal{G}(x, K) + \lambda(t)^T \left(x'(t) - f(x, K) \right) \right) dt,$$

where $\lambda(t)$ is the adjoint variable. Through integration by parts and optimality conditions, the gradient of J with respect to K is derived as:

$$\frac{dJ}{dK} = \int_0^{t_f} \left(\frac{\partial \mathcal{G}}{\partial K} + \lambda(t)^T \frac{\partial f}{\partial K} \right) dt,$$

where $\lambda(t)$ satisfies the adjoint system:

$$\begin{cases} \dfrac{d\lambda}{dt} = \dfrac{\partial \mathcal{G}}{\partial x} - \left(\dfrac{\partial f}{\partial x}\right)^T \lambda(t), \\ \lambda(t_f) = 0. \end{cases}$$

3.4. Derivation of the feedback gradient expressions

To implement the gradient descent algorithm described earlier, it is essential to compute the gradient of the objective function $J(k_1, k_2)$ with respect to the feedback weights k_1 and k_2. This subsection details the analytical derivation of these gradients using the adjoint sensitivity method.
The objective function to minimize is given by

$$J(k_1, k_2) = \int_0^{t_f} \left(I(t) - R(t) + \frac{1}{2} c_1 k_1^2 + \frac{1}{2} c_2 k_2^2 \right) dt.$$

Since $u(t)$ depends explicitly on k_1 and k_2, which in turn influence the system dynamics, we adopt a Lagrangian formulation. Let $\lambda(t)$ denote the adjoint vector associated with the state variables. The total derivative of the Lagrangian with respect to $K = (k_1, k_2)$ reads:

$$\frac{dJ}{dK} = \int_0^{t_f} \left(\frac{\partial \mathcal{G}}{\partial K} + \lambda(t)^\top \frac{\partial f}{\partial K} \right) dt,$$

where $\mathcal{G}$ is the running cost and f is the right-hand side of the controlled system.
First, we compute

$$\frac{\partial \mathcal{G}}{\partial k_1} = c_1 k_1, \quad \frac{\partial \mathcal{G}}{\partial k_2} = c_2 k_2,$$

from the explicit regularization terms.
Next, we evaluate $\frac{\partial f}{\partial K}$. Taking the partial derivatives with respect to k_1 and k_2, we obtain:

$$\frac{\partial f}{\partial k_1} = \begin{pmatrix} 0 \\ 0 \\ -\dfrac{AI}{D^2} \\ I\Big(I' - k_1 \dfrac{AI}{D^2}\Big) \end{pmatrix}, \quad \frac{\partial f}{\partial k_2} = \begin{pmatrix} 0 \\ 0 \\ -\dfrac{I^2}{D} \\ I\Big(I - k_1 \dfrac{I^2}{D}\Big) \end{pmatrix}.$$

The corresponding terms in the gradient expression become:

$$\lambda^\top \frac{\partial f}{\partial k_1} = \lambda_3\Big(-\frac{AI}{D^2}\Big) + \lambda_4 I\Big(I' - k_1 \frac{AI}{D^2}\Big), \quad \lambda^\top \frac{\partial f}{\partial k_2} = \lambda_3\Big(-\frac{I^2}{D}\Big) + \lambda_4 I\Big(I - k_1 \frac{I^2}{D}\Big).$$

Substituting into the Lagrangian derivative, we obtain the final gradient formulas:

$$\frac{dJ}{dk_1} = \int_0^{t_f} \Big[c_1 k_1 + \lambda_3\Big(-\frac{AI}{D^2}\Big) + \lambda_4 I\Big(I' - k_1 \frac{AI}{D^2}\Big) \Big] dt,$$

$$\frac{dJ}{dk_2} = \int_0^{t_f} \Big[c_2 k_2 + \lambda_3\Big(-\frac{I^2}{D}\Big) + \lambda_4 I\Big(I - k_1 \frac{I^2}{D}\Big) \Big] dt.$$

These expressions are used within the training algorithm to iteratively update the feedback weights, as described in Algorithm 1.

3.5. Gradient descent optimization algorithm

The optimal weights K are updated iteratively using the gradient descent method:

$$K_{j+1} = K_j - \eta \nabla_K J(x_j, K_j),$$

where η is the learning rate and $\nabla_K J$ is the gradient computed using the adjoint system. The full optimization procedure is summarized below (see Algorithm 1).

Algorithm 1: Gradient-Based Optimization of Feedback Control

Inputs: Initial condition x_0, learning rate η, tolerance ε.
Output: Optimal feedback weights $K = (k_1, k_2)$.

Initialize iteration counter $j = 0$, initial guess $K^0 = (k_1^0, k_2^0)$.
Compute initial control $u^0(t)$ using Eq (3.3).
Repeat until convergence or $j > j_{\max}$**:**

1. Solve the state system (3.1) forward in time to obtain $x_j(t)$.
2. Solve the adjoint system backward to compute $\lambda_j(t)$.
3. Compute the gradient $\nabla_K J(x_j, \lambda_j, K_j)$.
4. Update the weights: $K_{j+1} = K_j - \eta \nabla_K J(x_j, \lambda_j, K_j)$.
5. Update control $u^{j+1}(t)$ using updated weights.
6. Check convergence: **if** $\frac{\|u^{j+1} - u^j\|}{\|u^j\|} \leq \epsilon$ **stop**.
7. Increment $j \leftarrow j + 1$.

This framework ensures that the control strategy evolves intelligently with the epidemic dynamics, making it particularly suited for real-time policy adjustments and robust epidemic mitigation.

3.6. Numerical studies

In this section, we present numerically obtained results for solving our optimal problem (3.4), where in the first case we treat the evolution of the system without k_1, while in the second case we apply both controls in order to have a conclusion that solidifies our theoretical findings. The simulations are performed using the parameters $c_1 = 0.5$, $c_2 = 0.05$, learning rate $\eta = 10^{-3}$, and tolerance $\varepsilon = 10^{-6}$. The parameter values and the initial conditions used in these simulations are taken from [6, 15] and are summarized in Table 2.

Table 2. Values and interpretations of the parameters for our model.

Parameters	Interpretations	values
Λ	Coefficient of the recruitment rate	0.1
α	Infection rate coefficient	0.3
d	Coefficient of the natural mortality rate	0.1
r	Coefficient of the mortality due to the virus	0.003
a	The inverse of the average incubation period of the disease	1/12
g	Coefficient of the recovery intensity of infected individuals	1/14
θ	Loss rate of immunity	0.1

First, we simulate the system in the absence of any control intervention. This configuration represents the natural evolution of the epidemic and serves as a reference for our comparative analysis.

In this uncontrolled scenario (Figure 1), the infected population reaches a significant peak, and the recovery is relatively slow. Such an evolution underscores the necessity for timely and adaptive intervention strategies.

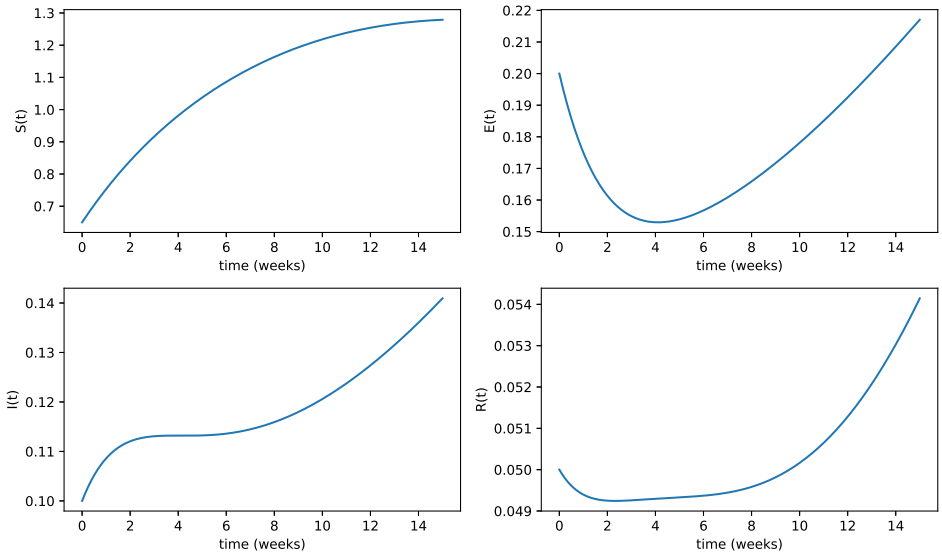

Figure 1. Population evolution in time without control.

3.7. Controlled dynamics using feedback control

Next, we apply our proposed feedback-based control strategy, defined as:

$$u(t) = k_1 I'(t) + k_2 I(t) = k_1 \frac{A(t)}{D(t)} + k_2 I(t),$$

with optimal weights k_1 and k_2 obtained via the gradient descent method.

As shown in Figure 2, the control feedback significantly reduces the infection peak and accelerates recovery. The control intensity adapts dynamically in response to epidemic trends, illustrating the benefits of including $I'(t)$ in the feedback loop.

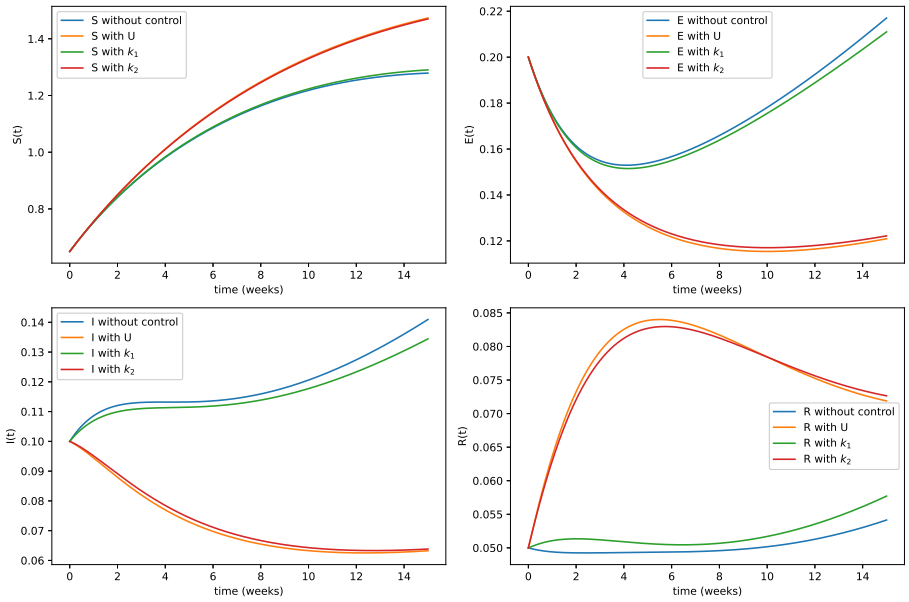

Figure 2. Population evolution in time with both controls.

4. Optimal control via Pontryagin's minimum principle

To complement the feedback-based control strategy previously developed, we now adopt a classical analytical approach grounded in Pontryagin's minimum principle (PMP) [3]. This method enables the determination of an optimal control trajectory by directly minimizing a predefined objective functional, subject to the dynamic constraints of the epidemiological system. In other biomedical situations, such as tumor-immune interaction models under therapeutic intervention, similar optimal-control formulations have been successfully implemented [23]. The use of PMP allows for a rigorous derivation of necessary conditions for optimality and offers a theoretical benchmark against which we can compare the feedback control policy.

4.1. Formulation of the optimal control problem

We reconsider the controlled SEIRS model under the influence of a scalar control $u(t)$ representing efforts such as treatment, isolation, or intensified healthcare interventions:

$$\begin{cases} S'(t) = \Lambda - \alpha S(t)I(t) - dS(t) + \theta R(t), \\ E'(t) = \alpha S(t)I(t) - (a+d)E(t), \\ I'(t) = aE(t) - (g+r+d+u(t))I(t), \\ R'(t) = (g+u(t))I(t) - (\theta+d)R(t). \end{cases} \tag{4.1}$$

Our goal is to identify the optimal control $u^*(t)$ minimizing the cost functional:

$$J(x(t), u(t)) = \int_0^{t_f} \left[I(t) - R(t) + \frac{1}{2} a_1 u(t)^2 \right] dt, \tag{4.2}$$

where the integrand balances the need to reduce infection levels while rewarding recovery, penalized by the quadratic cost associated with control application. The scalar $a_1 > 0$ tunes the intensity of this penalization.

The admissible controls are those functions $u(t)$ satisfying:

$$\mathcal{U} := \left\{u(t) : 0 \le u(t) \le 1,\ \forall t \in [0, t_f]\right\}.$$

Existence of an optimal control

Before deriving the necessary conditions, we establish the existence of at least one optimal control.

Theorem 4.1. *There exists a measurable control function $u^*(t) \in \mathcal{U}$ that minimizes the functional J, i.e.,*

$$J(u^*) = \min_{u \in \mathcal{U}} J(u).$$

Proof. The proof follows from standard results in optimal control theory, particularly those by Fleming and Rishel [1]. We verify the following assumptions:

- The set of admissible controls $\mathcal{U}$ is nonempty, convex, and closed.
- The right-hand side of the state system (4.1) is continuous and bounded in x and u, and satisfies Lipschitz conditions ensuring existence and uniqueness of solutions.
- The cost integrand $L(x, u) = I(t) - R(t) + \frac{1}{2}a_1u^2(t)$ is convex in u.
- There exist constants $c_3 \in \mathbb{R}$, $c_4 > 0$, and $n > 1$ such that $L(x, u) \ge c_3 + c_4\|u\|^n$, due to the quadratic term in u and boundedness of state variables.

Therefore, all required hypotheses are satisfied, and the existence of an optimal control is guaranteed by the theorem in [1]. □

4.2. Application of Pontryagin's principle

To characterize the optimal control $u^*(t)$, we invoke Pontryagin's minimum principle. Let $\lambda(t) = (\lambda_1(t), \lambda_2(t), \lambda_3(t), \lambda_4(t))$ be the adjoint variables associated with the state equations. The Hamiltonian function for this problem is defined as:

$$H = I(t) - R(t) + \frac{1}{2}a_1u(t)^2 + \sum_{i=1}^{4} \lambda_i(t) f_i(x(t), u(t)), \tag{4.3}$$

where f_i denotes the right-hand side of the *ith* equation in (4.1). The adjoint system is then given by:

$$\begin{cases} \lambda_1'(t) = (\alpha I(t) + d)\lambda_1(t) - \alpha I(t)\lambda_2(t), \\ \lambda_2'(t) = (a + d)\lambda_2(t) - a\lambda_3(t), \\ \lambda_3'(t) = -1 + \alpha S(t)(\lambda_1(t) - \lambda_2(t)) + (g + r + d + u(t))\lambda_3(t) - (g + u(t))\lambda_4(t), \\ \lambda_4'(t) = 1 - \theta\lambda_1(t) + (\theta + d)\lambda_4(t), \end{cases} \tag{4.4}$$

with the transversality conditions:

$$\lambda_i(t_f) = 0, \quad \text{for } i = 1, 2, 3, 4.$$

Characterization of the optimal control

The optimal control $u^*(t)$ is obtained by minimizing the Hamiltonian with respect to u, i.e.,

$$u^*(t) = \arg\min_{u\in[0,1]} H(x(t), u, \lambda(t)).$$

Setting the derivative of H with respect to u to zero and projecting onto the admissible set, we obtain:

$$u^*(t) = \min\left(1, \max\left(0, \frac{\lambda_3(t) - \lambda_4(t)}{a_1} I(t)\right)\right). \tag{4.5}$$

This feedback form of the optimal control links it explicitly to the state variable $I(t)$ and the adjoint variables $\lambda_3(t)$ and $\lambda_4(t)$, offering a direct means for implementation once the forward and backward systems are solved.

Proof. The derivation follows directly from Pontryagin's conditions:

$$\lambda_i'(t) = -\frac{\partial H}{\partial x_i}, \quad \text{and} \quad \frac{\partial H}{\partial u} = a_1 u(t) + I(t)(\lambda_3(t) - \lambda_4(t)) = 0.$$

Solving this equation gives:

$$u(t) = \frac{\lambda_3(t) - \lambda_4(t)}{a_1} I(t),$$

which is then projected onto the admissible control set $[0, 1]$ to obtain (4.5). □

4.3. Numerical implementation and simulation results

To numerically evaluate the optimal control derived via Pontryagin's minimum principle, we solve the associated optimality system, which consists of the state equations, adjoint equations, and the control characterization. This forms a two-point boundary value problem (TPBVP), with initial conditions imposed on the state variables and terminal conditions specified for the adjoint variables.

The resolution proceeds iteratively: We begin with an initial guess for the control $u(t)$, then solve the state system forward in time, followed by a backward integration of the adjoint system. The control is subsequently updated using the characterization formula (4.5), and the process is repeated until convergence of successive control profiles is achieved. All simulations were performed using Python, with numerical parameters and initial conditions consistent with those used in previous sections. The resulting population trajectories under Pontryagin's minimum principle are shown in Figure 3.

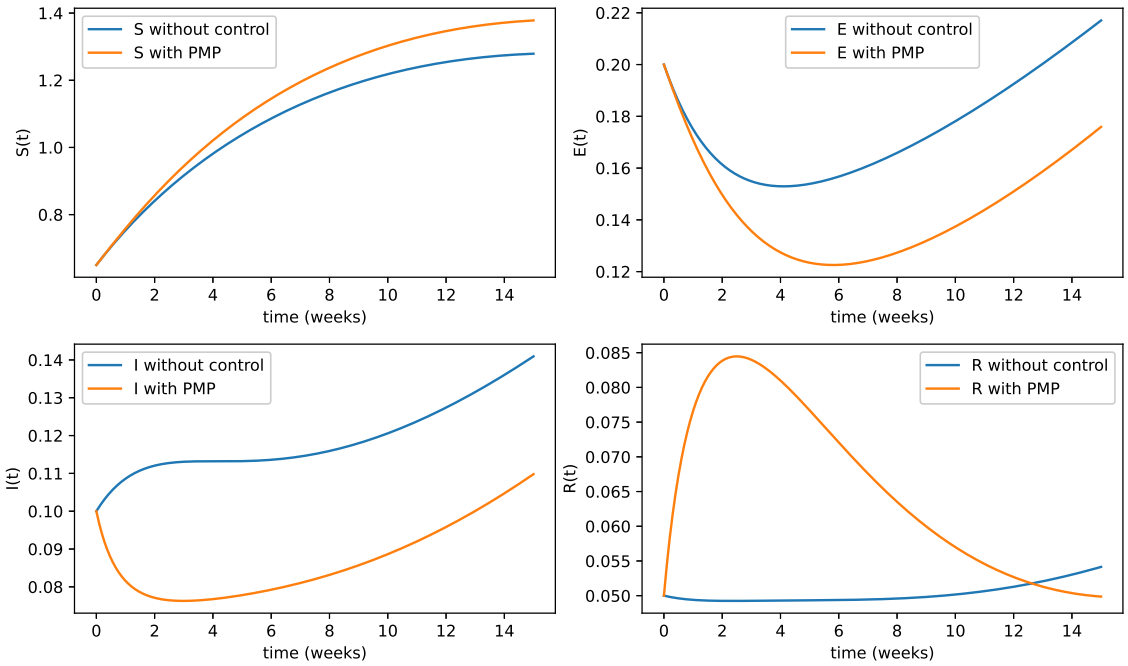

Figure 3. Population dynamics using Pontryagin's minimum principle.

This approach produces an optimal trajectory based on backward-forward integration. While PMP yields a viable solution, the resulting control may lack responsiveness to rapid epidemic surges.

Comparative assessment of control strategies

To evaluate the relative performance of the two proposed control approaches, the feedback-based strategy and the Pontryagin-derived optimal control, we focus on the infected and recovered compartments, which offer the most direct insights into the epidemic's progression and containment effectiveness.

Figure 4 illustrates the temporal evolution of the population under the two controls laws:

- **Feedback Control :** This strategy, defined by $u(t) = k_1(t)I'(t) + k_2(t)I(t)$, achieves a significant reduction in the infection peak and a notable increase in the number of recovered individuals. The dynamic nature of this control, reacting to both the state and its rate of change, enables rapid adjustments in response to epidemic acceleration.
- **Pontryagin's Optimal Control:** Although effective in dampening the epidemic curve, this strategy results in a higher infection peak and a comparatively lower number of recoveries. The control profile tends to be smoother but less responsive to sudden changes in infection growth.

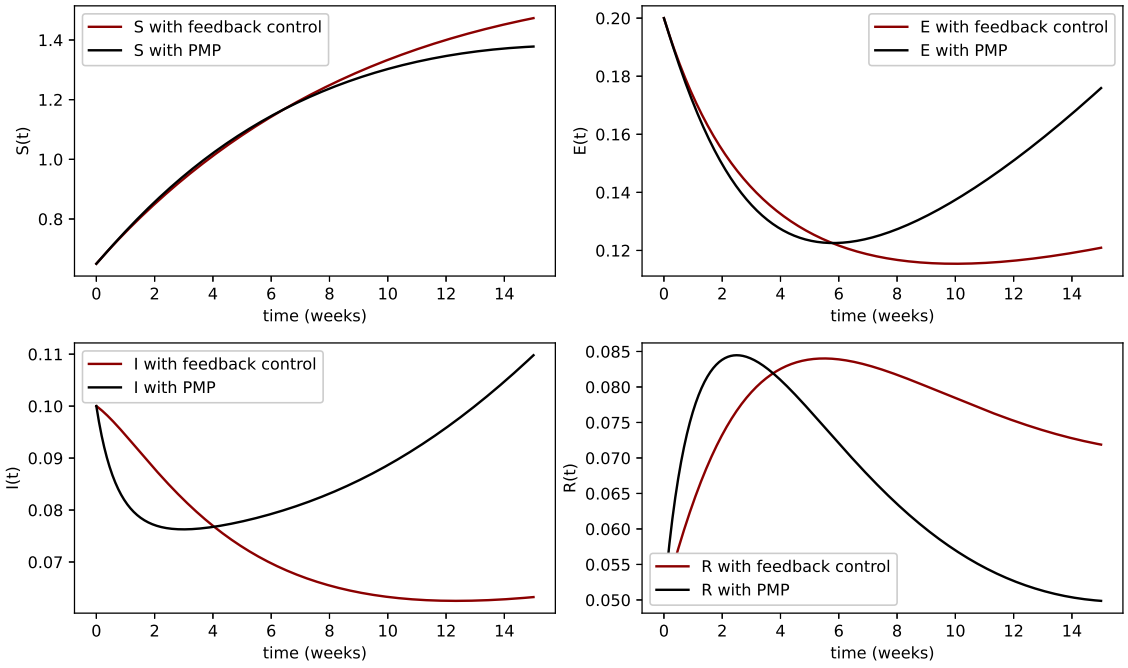

Figure 4. Comparison of infection and recovery between feedback and PMP control strategies.

The comparison clearly indicates that the feedback control strategy outperforms the classical optimal control in both reducing the disease burden and accelerating recovery. Its reliance on real-time epidemic signals ($I(t)$ and $I'(t)$) makes it a more robust and adaptive tool, especially in scenarios where rapid fluctuations in infection rates occur. These results advocate for the integration of such feedback mechanisms into epidemic response frameworks, offering enhanced responsiveness over traditional control optimization methods.

5. Conclusions

In this work, we have developed and analyzed an enhanced SEIRS epidemic model incorporating a dynamic feedback control strategy based on both the current level of infection $I(t)$ and its rate of change $I'(t)$. This dual-dependence control law introduces a higher degree of responsiveness to changes in epidemic dynamics, enabling more timely and effective interventions.

To assess the efficiency of the proposed approach, we formulated an optimization problem and applied adjoint sensitivity analysis combined with gradient descent techniques to identify the optimal feedback parameters. Furthermore, we conducted a rigorous comparison with a classical optimal control strategy derived from Pontryagin's minimum principle. Numerical simulations have shown that the feedback-based control outperforms the Pontryagin-based approach in reducing infection peaks and enhancing the recovery process, offering a more robust framework for real-time epidemic management.

These findings highlight the potential of adaptive, data-driven control strategies in public health planning, especially in rapidly evolving epidemic contexts. Future research directions may include calibrating the model using empirical data, extending it to spatial or network-based structures, and

integrating more realistic features such as time delays, age structures, vaccination dynamics or fractional order versions [24]. Such extensions would further enhance the model's applicability to real-world epidemic control scenarios.

Author contributions

Mohammed Azoua: Formal analysis, investigation, resources, writing – original draft, validation, and data curation; Marouane Karim: Formal analysis, investigation, writing – review and editing; Amine Rachih: Formal analysis, investigation, writing – review and editing; Mostafa Rachik: Formal analysis, investigation, writing – review and editing; Mahmoud Zaky: Project administration, methodology, writing – review and editing, and formal funding acquisition. All authors have read and approved the final version of the manuscript for publication.

Use of Generative-AI tools declaration

The authors declare they have not used Artificial Intelligence (AI) tools in the creation of this article.

Conflict of interest

The authors declare there is no conflict of interest.

References

1. W. H. Fleming, R. W. Rishel, *Deterministic and stochastic optimal control*, J. R. Stat. Soc. A (General), Springer-Verlag, New York, **139** (1975). https://doi.org/10.2307/2344363
2. W. O. Kermack, A. G. McKendrick, A contribution to the mathematical theory of epidemics, *Proc. R. Soc. Lond. A.*, **115** (1927), 700–721. https://doi.org/10.1098/rspa.1927.0118
3. L. S. Pontryagin, V. G. Boltyanskii, R. V. Gamkrelidze, E. F. Mishchenko, *The mathematical theory of optimal processes*, New York-London, 1962. https://doi.org/10.1002/zamm.19630431023
4. O. P. Agrawal, A general formulation and solution scheme for fractional optimal control problems, *Nonlinear Dyn.*, **38** (2004), 323–337. https://doi.org/10.1007/s11071-004-3764-6
5. O. P. Agrawal, O. Defterli, D. Baleanu, Fractional optimal control problems with several state and control variables, *J. Vib. Control*, **16** (2010), 1967–1976. https://doi.org/10.1177/1077546309353361
6. M. Azoua, M. Karim, A. Azouani, I. Hafidi, Improved parameter estimation in epidemic modeling using continuous data assimilation methods, *J. Appl. Math. Comput.*, **70** (2024), 1–26. https://doi.org/10.1007/s12190-024-02145-w
7. A. Khan, G. Zaman, Optimal control strategies for an age-structured SEIR epidemic model, *Math. Method. Appl. Sci.*, **45** (2022), 8701–8717. https://doi.org/10.1002/mma.7823

8. M. De la Sen, S. Alonso-Quesada, A. Ibeas, On the stability of an SEIR epidemic model with distributed time-delay and a general class of feedback vaccination rules, *Appl. Math. Comput.*, **270** (2015), 953–976. https://doi.org/10.1016/j.amc.2015.08.099
9. X. Lü, H. W. Hui, F. F. Liu, Y. L. Bai, Stability and optimal control strategies for a novel epidemic model of COVID-19, *Nonlinear Dynam.*, **106** (2021),1491–1507. https://doi.org/10.1007/s11071-021-06524-x
10. E. Hansen, T. Day, Optimal control of epidemics with limited resources, *J. Math. Biol.*, **62** (2011), 423–451. https://doi.org/10.1007/s00285-010-0341-0
11. L. Bolzoni, E. Bonacini, C. Soresina, M. Groppi, Time-optimal control strategies in SIR epidemic models, *Math. Biosci.*, **292** (2017), 86–96. https://doi.org/10.1016/j.mbs.2017.07.011
12. M. Karim, A. Kouidere, M. Rachik, K. Shah, T. Abdeljawad, Inverse problem to elaborate and control the spread of COVID-19: A case study from Morocco, *AIMS Math.*, **8** (2023), 23500–23518. https://doi.org/10.3934/math.20231194
13. S. Cacace, A. Oliviero, Reliable optimal controls for SEIR models in epidemiology, *Math. Comput. Simul.*, **223** (2024), 523–542. https://doi.org/10.1016/j.matcom.2024.04.034
14. H. J. Lee, Robust observer-based output-feedback control for epidemic models: Positive fuzzy model and separation principle approach, *Appl. Soft Comput.*, **132** (2023), 109802. https://doi.org/10.1016/j.asoc.2022.109802
15. M. Azoua, A. Azouani, I. Hafidi, Optimal control and global stability of the SEIQRS epidemic model, *Commun. Math. Biol. Neu.*, 2023. https://doi.org/10.28919/cmbn/7880
16. A. Kouidere, L. E. Youssoufi, H. Ferjouchia, O. Balatif, M. Rachik, Optimal control of mathematical modeling of the spread of the COVID-19 pandemic with highlighting the negative impact of quarantine on diabetics people with cost-effectiveness, *Chaos Soliton. Fract.*, **145** (2021), 110777. https://doi.org/10.1016/j.chaos.2021.110777
17. U. Boscain, M. Sigalotti, D. Sugny, Introduction to the Pontryagin maximum principle for quantum optimal control, *PRX Quantum*, **2** (2021), 030203. https://doi.org/10.1103/PRXQuantum.2.030203
18. E. Jung, S. Iwami, Y. Takeuchi, T. C. Jo, Optimal control strategy for prevention of avian influenza pandemic, *J. Theor. Biol.*, **260** (2009), 220–229. https://doi.org/10.1016/j.jtbi.2009.05.031
19. K. Blayneh, Y. Cao, H. D. Kwon, Optimal control of vector-borne diseases: Treatment and prevention, *Discrete Cont. Dyn-S.*, **11** (2009), 587–611. https://doi.org/10.3934/dcdsb.2009.11.587
20. K. Sarkar, S. Khajanchi, J. J. Nieto, Modeling and forecasting the COVID-19 pandemic in India, *Chaos Soliton. Fract.*, **139** (2020), 110049. https://doi.org/10.1016/j.chaos.2020.110049
21. S. Khajanchi, K. Sarkar, J. Mondal, K. S. Nisar, S. F. Abdelwahab, Mathematical modeling of the COVID-19 pandemic with intervention strategies, *Results Phys.*, **25** (2021), 104285. https://doi.org/10.1016/j.rinp.2021.104285
22. R. K. Rai, S. Khajanchi, P. K. Tiwari, E. Venturino, A. K. Misra, Impact of social media advertisements on the transmission dynamics of COVID-19 pandemic in India, *J. Appl. Math. Comput.*, 2022, 1–26. https://doi.org/10.1007/s12190-021-01507-y

23. S. Khajanchi, Stability analysis of a mathematical model for glioma-immune interaction under optimal therapy, *Int. J. Nonlin. Sci. Num.*, **20** (2019), 269–285. https://doi.org/10.1515/ijnsns-2017-0206

24. S. S. Ezz-Eldien, E. H. Doha, Y. Wang, W. Cai, A numerical treatment of the two-dimensional multi-term time-fractional mixed sub-diffusion and diffusion-wave equation, *Commun. Nonlinear Sci. Numer. Simul.*, **91** (2020), 105445. https://doi.org/10.1016/j.cnsns.2020.105445

AIMS Press